UDC 539.4

Effect of the Surface Texture on Laser Joining of a Carbon Fiber-Reinforced Thermosetting Plastic and Stainless Steel

L. Y. Sheng,[a,1] C. Lai,[a] Z. Xu,[b] and J. Jiao[b]

[a] Shenzhen Institute, Peking University, Shenzhen, China

[b] Ningbo Institute of Materials Technology and Engineering, Chinese Academy of Sciences, Ningbo, China

[1] lysheng@yeah.net

A carbon fiber-reinforced thermosetting plastic and stainless steel were joined by the fiber laser. The surface texture effect on the joint was investigated. The abrasive paper scratching is shown to form single directional striae on stainless steel with intermittent ridges. Laser texture processing creates uniformly distributed microdimples and ridges, which forms a rectangular cellular structure. This processing can improve the fluidity of molten polyphenylene sulfite during laser joining. Laser scanning on stainless steel results in the formation of fusion and heat-affected zones. In the heat-affected zone, lathy ferrite is located along the boundary, while in the fusion zone, ferrite forms the skeletal structure and separates austenite into a cellular structure. The surface texture modification can contribute to the adhesive strength between stainless steel and polyphenylene sulfite through on enlarged contact surface area by forming striae, microdimples, and ridges. As compared to the abrasive paper scratching, the stainless steel/plastic joint with laser texture processing exhibits a higher shear strength.

Keywords: laser joining, carbon fiber-reinforced thermosetting plastic (CFRTP), stainless steel, microstructure, surface texture.

Introduction. Recently, the carbon fiber reinforced polymer (CFRP) has received a great attention, because of its advantages, such as high specific stiffness, excellent corrosion resistance, high strength to weight ratios and good environmental degradation etc. [1]. Therefore, it has been applied as the structural material in many fields, such as aerospace, automotive, concrete structure and so on [2, 3]. However, during the application of CFRP, it is inevitable to encounter the problem how to join CFRP with metal based components. The mechanical joining is a convenient way with high efficiency [4]. However, due to the characteristics of the CFRP, the conventional mechanical joining could not join the CFRP on metal without the damage on carbon fiber [5]. The research on the double-lap joints of aluminum and CFRP laminate by rivets arrays exhibited that the initial delamination near the CFRP hole edge could promote the propagation of crack or delamination [6]. The previous research [7] showed that the adhesive bonding could join the CFRP and metal without any damage on the CFRP, but the long cure processing, high cost, low bonding strength restricted its application. Therefore, it is necessary to develop the processing technology without damage on carbon fiber and polymer.

The polyphenylene sulfite (PPS) based carbon fiber reinforced thermoplastic (CFRTP) is a kind of carbon fiber reinforced polymer with good thermo-process feature and the main advantages of CFRP, so it can be joined with the metal by thermal processing. The recent study exhibited the CFRTP and metal could be joined together by friction stir method, which took use of heat from the friction stirring metal to melt the CFRTP and fix metal and CFRTP [8]. Though the friction stir could decrease the damage of the CFRTP, the stress would concentrate along the friction stirred hole and then lead to the failure of the CFRTP. Therefore, a kind of processing method is needed to join the CFRTP and metal with less effect on the joint. Katayama and Kawahito [9] exhibited that the direct laser irradiate on stainless steel could generate a Cr_2O_3 transition layer on interface of plastic/stainless steel.

© L. Y. SHENG, C. LAI, Z. XU, J. JIAO, 2019

Moreover, the research of Tan et al. [10] revealed that the existence of Cr layer on the steel surface enhanced the shear strength of the CFRP/steel joint by the Cr-O-PA6T bonding along joint interface. In addition, the recent research demonstrated that the machined microgrooves on the metal surface increased the strength of laser joining plastic/aluminum joint to 24 MPa [11]. However, the plastic without strengthening fiber could not represent the typical CFRTP, since the presence of carbon fiber influenced the heat transfer. Moreover, the microdimples on metal surface might lead to the formation of air bubbles in the joint. It was necessary to investigate the effect of surface morphology on laser joining of CFRTP and metal. Therefore, the stainless with different surface morphology was fabricated and joined with CFRTP by fiber laser in the present research. Moreover, microstructure and morphology of stainless steel, joint interface and shear strength of the joint were investigate.

1. **Experimental Procedures**. In the present study, the CFRTP panels with PPS matrix reinforced by T700 carbon fibers were cut into the size of 50×30×3 mm. The CFRTP is composed by PPS matrix and 15 layers T700 carbon fibers, which is weaved with intersected structure. The carbon fiber is wrapped by the PPS and the average thickness of single layer is 200 μm. The 304 stainless steel specimens with size of 50×30×2 mm were prepared. Some stainless steel plates were scratched by the 400# abrasive paper to increase the roughness, and some stainless steel plates were processed by laser to form the surface texture. Table 1 presents the chemical composition of the 304 stainless steel.

Table 1

Chemical Composition of the 304 Stainless Steel (wt.%)

C	Mn	Si	Ni	Cr	S	P	Fe
0.07	0.78	0.56	8.10	18.33	0.006	0.032	Balanced

The joining of stainless steel and CFRTP was conducted by a fiber laser welding system. This system comprises 1410RABB robot, 500 W fiber laser (continuous wave laser machine and the wavelength is 1080 nm), laser processing head (the focal length is 120 mm), air-actuated clamp and cooling system [12]. Firstly, the CFRTP overlaid with PPS additive on surface was placed on the laser welding system and the stainless steel plate was placed above the PPS additive. After then, the stainless steel, PPS additive and CFRTP were clamped by the air-actuated clamp which had a groove with size of 60×10×5 mm in the upper one. The clamping pressure could be adjusted by controlling the air-actuator. During the laser joining, the laser beam would scan on the surface of stainless steel in the groove with the argon gas flow velocity of 30 l/min. The laser power, laser scanning speed, clamping pressure, and thickness of PPS additive were 320 W, 5 mm/s, 0.5 MPa, and 200 μm, respectively. The defocusing distance was −20 mm and the laser beam diameter was 500 μm.

The specimen for cross-sectional observation was cut from the stainless steel and CFRTP joint and polished by the conventional metallographic method. The KEYENCE VX-X200 CLSM was employed to analyze the surface of the stainless steel. The Phenom Pro SEM was employed to observe the microstructure of laser scanned stainless steel and the morphology of joint interface. In the present research, the tensile test was performed on the UTM4304 electronic universal testing machine to obtain the shear strength. The shear strength test was referred to the GB/T7124-86 and ASTM F2255-2005(2010) standards. The tensile tests were carried out in air with the initial strain rate of $2 \cdot 10^{-3}$ s^{-1} at room temperature. Three specimens were tested under the same conditions to obtain the shear strength data. The Stemi 2000 OM was applied to observe the debonding surface of tensile specimens.

2. **Results and Discussion**. The morphology of the stainless steel scratched by the abrasive paper is shown in Fig. 1. It can be found that the short-time processing by abrasive paper has formed the furrows with the same directions, as shown in Fig. 1a. Moreover, the furrows are stopped by the promontory intermittently. The surface morphology analyzed by the CLSM exhibits that the furrows and promontory distribute irregularly, as shown in Fig. 1b. The calculated roughness of the abrasive paper scratch stainless steel is about 0.7 μm. Further observations on the stainless steel scratched by abrasive paper reveal that the size of the furrow differs greatly, as shown in Fig. 1c, d. It can be found that the stainless steel surface has experienced obvious deformation. There are rheology features along the ridge and stripping pits also demonstrate the crack failure with high stress concentration. The surface topography analysis also exhibits existence of promontory and the difference of the furrows.

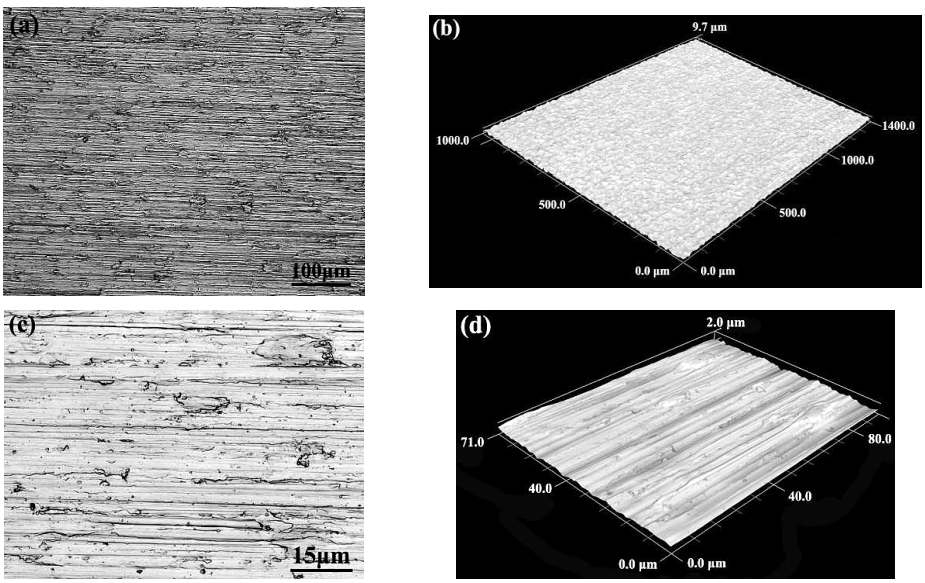

Fig. 1. Morphology of the stainless steel surface scratched by abrasive paper: (a) low magnification; (b) surface topography analysis of (a); (c) high magnification; (d) surface topography analysis of (c).

The observation results of the laser-processed stainless steel are visualized in Fig. 2. Clearly, the laser processing has generated uniform texture on the stainless steel surface, as shown in Fig. 2a. The microdimples and ridges distribute uniformly and exhibit rectangular array structure. The size of the microdimple ranges from 5×10 to 15×25 μm. The surface topography analysis confirms the existence of regular distribution of microdimples and ridges, as shown in Fig. 2b. The calculated roughness of the laser processed stainless steel is about 6 μm. The further observation on the laser processed stainless steel reveals that there is obvious metallurgical behavior, as shown in Fig. 2c. The lath-like microstructure on the surface of ridges demonstrates the happening of phase transformation, which may be attributed to the rapid solidification during the laser processing. According to previous researches [13], the rapid solidification could result in the formation of martensitic phase. The surface topography analysis reveals that the depths of the microdimples are quite similar, as shown in Fig. 2d.

The typical microstructures of PPS based CFRTP and PPS additive are shown in Fig. 3. Clearly, the PPS-based CFRTP is mainly composed of black-grey carbon fibers and white-grey PPS matrix, as shown in Fig. 3a. The carbon fibers are overlapped layer-by-layer, while most carbon fibers are packed and bonded together by PPS. Based on the

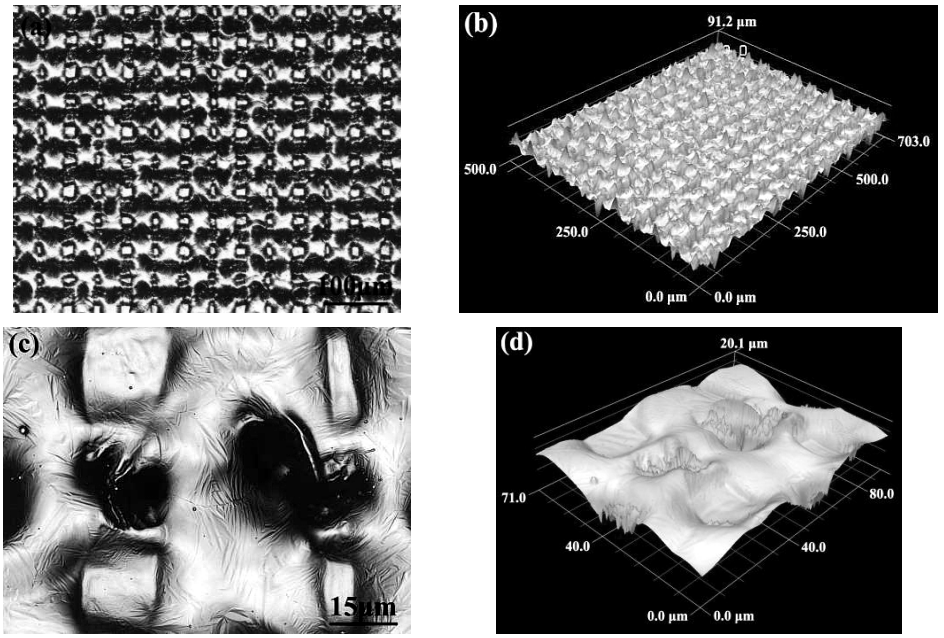

Fig. 2. Morphology of the stainless steel surface texture processed by laser: (a) low magnification; (b) surface topography analysis of (a); (c) high magnification; (d) surface topography analysis of (c).

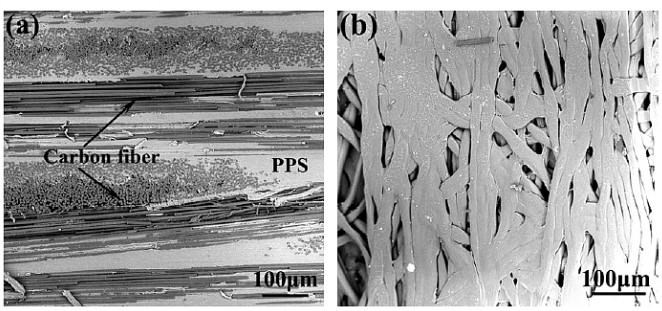

Fig. 3. Morphology of the PPS based CFRTP and PPS additive: (a) morphology of the CFRTP with the overlapping of carbon fibers; (b) morphology of the PPS additive.

macroscopic observation, carbon fibers are weaved as decussate structure. The layer of carbon fiber is about 200 μm in thickness. The observation on the layer of carbon fiber shows that they have the average size of 6 μm in diameter. The observation on the torn PPS based CFRTP exhibits that the carbon fiber has good integrity with regular arrangement. The SEM observation on the PPS additive reveals that the wires of PPS are overlapped randomly and there is relative high porosity, as shown in Fig. 3b. Based on the SEM image, the PPS wire has the size of 20–30 μm in diameter.

The macrograph of the laser-processed stainless steel/CFRTP joint is shown in Fig. 4. Clearly, the laser scanning results in the ignited feature in the stainless steel which has obvious oxidation on the track of laser scanning, as shown in Fig. 4a. The observation on the interface of the laser-joined CFRTP and stainless steel reveals that the morphology of stainless steel could exert some influence on the fluidity of PPS additive. The abrasive paper scratched stainless steel contributes little on the fluidity of PPS additive, as shown in Fig. 4b. Such a phenomenon may be attributed to the small size and single direction of the furrow on the stainless steel. The texture processed by laser on the stainless steel improves

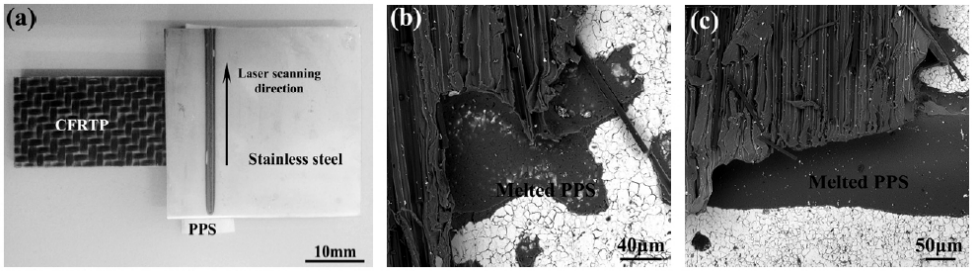

Fig. 4. (a) Macrophotograph of the stainless steel/CFRTP joint; (b) morphology of the joint interface with scratched surface by abrasive paper; (c) morphology of the joint interface with surface texture.

the fluidity of PPS additive, as shown Fig. 4c. It can be seen that some melted PPS additive has flowed out of the gap and spread on the adjacent stainless steel, which may be attributed to the rectangular array structure formed by the microdimples and ridges. According to the recent research [12], the laser scanned surface of the steel would reach 1800 μm and the interface of the stainless steel and CFRTP would reach 400 μm. That indicates the heat from the laser scanning would be exceeded for the melting of the PPS additive. Then it can ensure the PPS additive and the surface of the CFRTP would be merged with each other and then bonded with the stainless steel. Therefore, the roughness of the stainless steel surface is helpful to increase the bonding surface and improve the bonding strength.

The observation on the laser scanned stainless steel reveals that the laser scanning influences the microstructure greatly, as shown in Fig. 5. It can be seen that there are fusion zone and heat-affect zone in the steel, which exhibits hemi-ellipsoidal shape, as shown in Fig. 5a. The fusion zone is marked by the blue dash line and has the width of about 370 μm and the depth of about 430 μm. The heat-affected zone embraces the fusion zone and has the width of 60–140 μm, which is marked between the red dash line and blue dash line. Such morphologies of fusion and heat-affected zones should be attributed to the focus position of laser. Based on the microstructure analysis, it can be found that the stainless steel exhibits homogeneous grain structure with the average size of 20 μm, but the laser scanning changes the microstructure, as shown in Fig. 5b, c. In the heat-affected zone, the lathy ferrite mainly precipitates along the original grain boundary or twin boundary, which separates the original grain and refines the structure. With the observation proceeding to the fusion zone, the ferrite becomes coarse and increases, which forms the skeletal structure. In the fusion zone, the skeletal ferrite and cellular austenite is the main characteristic, as shown in Fig. 5d. Based on the researches [14–16], the microstructure of the fusion zone and heat-affect zone could be influenced by cooling rate. The higher cooling rate results in the formation of cellular structure. In the present research, the relative high Cr content and rapid laser scanning speed would promote the formation of ferrite with intercellular or interdentritic structure. Therefore, one can see the skeletal ferrite separates the austenite into small cells. Such a refined structure could contribute to the improvement of strength [17, 18].

In order to investigate the effect of stainless steel surface morphology on the bonding force of stainless steel/CFRTP joint, the shear strength of the joints were tested, as shown in Fig. 6. The stainless steel/CFRTP joint with abrasive paper scratching processing obtains the shear strength of 14.6 MPa, which is a little higher than that without any surface treatment [12]. While the laser texture processing increase the shear strength of the stainless steel/CFRTP joint to 20.6 MPa. The increased shear strength should be attributed the furrows, microdimples, and ridges formed on the stainless steel surface, because these microstructures increase the amount of contact surface area. Higher contact surface area

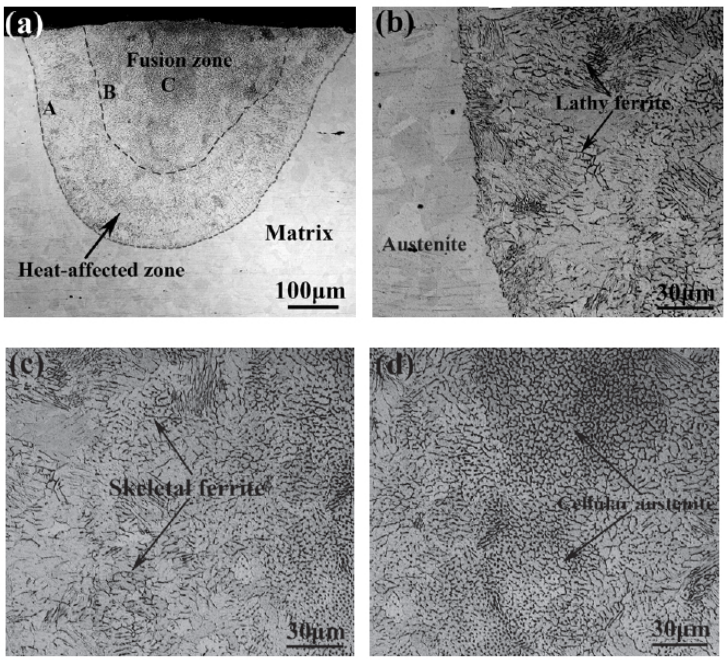

Fig. 5. Microstructure of the laser-scanned stainless steel: (a) macrophotograph of heat-affected zone and fusion zone; (b) lathy ferrite along the interface of matrix and heat-affected zone (*A* position); (c) skeletal ferrite along the fusion zone boundary (*B* position); (d) skeletal ferrite and cellular austenite in fusion zone (*C* position).

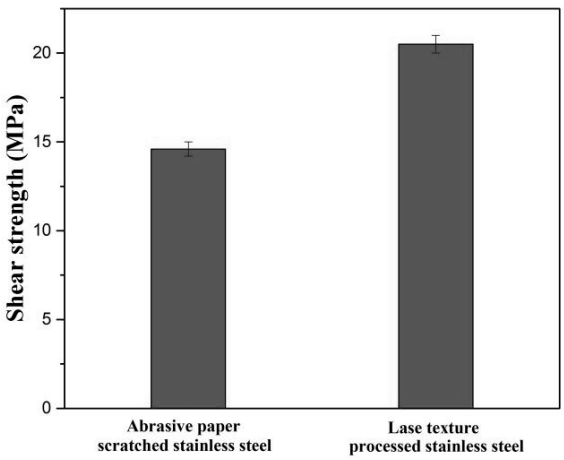

Fig. 6. The shear strength of the stainless steel/CFRTP joints with different stainless steel surface morphology.

between stainless steel and PPS additive means higher adhesive strength. Compared with the abrasive paper scratching, the laser texture processing could increase the contact surface area obviously by adjusting the depth of microdimple. Therefore, the stainless steel/CFRTP joint treated by laser texture processing has a higher shear strength.

The observations on the debonding surface of stainless steel/CFRTP joints show that the fracture mainly extend along the interface of PPS and carbon fiber layer, as shown in Fig. 7. However, the stainless steel surface morphology influences the fraction of carbon

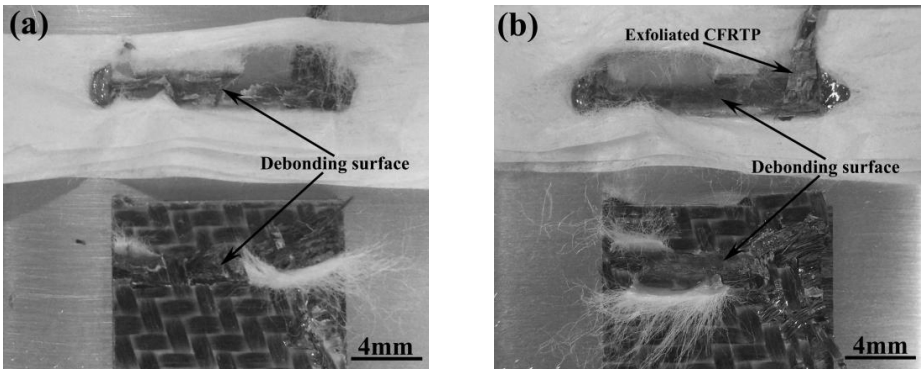

Fig. 7. Debonding surface of the stainless steel/CFRTP joints with different stainless steel surface morphology: (a) scratched by abrasive paper; (b) surface texture processed by laser.

fiber exfoliated from the CFRTP. As shown in the figure, on the debonding surface of joint with abrasive paper scratching only few carbon fiber is torn from the CFRTP, but on the on the debonding surface of joint with laser processing texture the bulk carbon fiber layer is torn from the CFRTP. Such a feature indicates the laser processing texture has increased the adhesion between stainless steel and CFRTP by the well coalesced PPS additive.

According the recent studies [19–21], the joining between the dissimilar materials is mainly depended on the initial mechanical bonding. In the present paper, the initial interface bonding of stainless steel/CFRTP joint includes the PPS/CFRTP and PPS/stainless steel. Then the surface morphology of stainless steel would play an important role, which determines the contact surface area and adhesion between stainless steel and PPS additive. Moreover, the research [6] also reveals that the thermal joining would promote the metal element diffusion from the stainless steel to melted PPS, which forms the new ion bond with the molecular bond of PPS and improves the bonding strength between the stainless steel and CFRTP. To achieve such a objective, the melted PPS should be attached to the stainless steel closely and cooperated with some additive. Therefore the contact surface area between the stainless steel and PPS become so important, which could determine the interface adhesive strength and influence the shear strength. The laser texture processing treatment could increase the contact surface area and increase the adhesive strength between stainless steel and PPS. Moreover, the increased contact surface area also promotes the increase of ion bond. Therefore, the laser texture processing could improve the shear strength of the stainless steel/CFRTP joint. Furthermore, the laser texture processing forms the cross-linking structure, which is beneficial to the flow of melted PPS and help the uniform distribution of PPS additive. The well-distributed melted PPS additive between the stainless steel and CFRTP also contributes to the improvement of the shear strength. Therefore, the stainless steel/CFRTP joint with laser texture processing treatment obtains a better shear strength value.

Conclusions

1. The abrasive paper scratching could generate the single directional furrows on the stainless steel with intermittent break by promontories. The laser texture processing forms the uniformly distributed microdimples and ridges. The laser texture processing could improve the fluidity of the melted PPS during laser joining.

2. The laser scanning on the stainless steel forms the fusion zone and heat-affected zone. In the heat-affected zone, the lathy ferrite precipitates along the boundary, while in the fusion zone, the ferrite forms the skeletal structure and separates the austenite into small cellular structure.

3. The abrasive paper scratching and laser texture processing could improve the shear strength of the stainless steel/CFRTP joint, which should be ascribed to the increased contact surface area by forming furrow, microdimple and ridge. Compared with the abrasive paper scratching, the stainless steel/CFRTP joint with laser texture processing obtains a better shear strength.

Acknowledgments. The authors are grateful to the support of Shenzhen Basic Research Project (JCYJ20150529162228734, JCYJ20170815153143221, JCYJ20150625155931806, JCYJ20160427100211076 and JCYJ20160427170611414, JCYJ20170306141506805).

1. X. L. Zhao and L. Zhang, "State-of-the-art review on FRP strengthened steel structures," *Eng. Struct.*, **29**, No. 8, 1808–1823 (2007).
2. G. Williams, R. Trask, and I. Bond, "A self-healing carbon fiber reinforced polymer for aerospace applications," *Compos. Part A-Appl. S.*, **38**, No. 6, 1525–1532 (2007).
3. A. Mayyas, A. Qattawi, M. Omar, and D. Shan, "Design for sustainability in automotive industry: a comprehensive review," *Renew. Sust. Energ. Rev*., **16**, No. 4, 1845–1862 (2012).
4. Z. Zhang, J. Shan, X. Tan, and J. Zhang, "Improvement of the laser joining of CFRP and aluminum via laser pre-treatment," *Int. J. Adv. Manuf. Tech.*, **90**, Nos. 9–12, 3465–3472 (2017).
5. F. Lambiase and D.-C. Ko, "Two-steps clinching of aluminum and Carbon Fiber Reinforced Polymer sheets," *Compos. Struct.*, **164**, 180–188 (2017).
6. G. Marannano and B. Zuccarello, "Numerical experimental analysis of hybrid double lap aluminum-CFRP joints," *Compos. Part B-Eng.*, **71**, 28–39 (2015).
7. P. Molitor, V. Barron, and T. Young, "Surface treatment of titanium for adhesive bonding to polymer composites: a review," *Int. J. Adhes. Adhes.*, **21**, No. 2, 129–136 (2001).
8. S. M. Goushegir, "Friction spot joining (FSpJ) of aluminum-CFRP hybrid structures," *Weld. World*, **60**, No. 6, 1073–1093 (2016).
9. S. Katayama and Y. Kawahito, "Laser direct joining of metal and plastic," *Scripta Mater.*, **59**, No. 12, 1247–1250 (2008).
10. X. Tan, J. Shan, J. Ren, "Effects of Cr plating layer on shear strength and interface bonding characteristics of mild steel/CFRP joint by laser heating," *Acta Metall. Sin*., **49**, 751–756 (2013).
11. A. Roesner, A. Olowinsky, and A. Gillner, "Long term stability of laser joined plastic metal parts," *Phys. Procedia*, **41**, 169–171 (2013).
12. J. Jiao, Z. Xu, Q. Wang, et al., "CFRTP and stainless steel laser joining: Thermal defects analysis and joining parameters optimization," *Opt. Laser Technol.*, **103**, 170–176 (2018).
13. M. Mukherjee, T. K. Pal, "Evaluation of microstructural and mechanical properties of Fe-16Cr-1Ni-9Mn-0.12N austenitic stainless steel welded joints," *Mater. Charact.*, **131**, 406–424 (2017).
14. L. J. Wang, L. Y. Sheng, and C. M. Hong, "Influence of grain boundary carbides on mechanical properties of high nitrogen austenitic stainless steel," *Mater. Design*, **37**, 349–355 (2012).
15. L. Y. Sheng, F. Yang, T. F. Xi, et al., "Microstructure and elevated temperature tensile behaviour of directionally solidified nickel based superalloy," *Mater. Res. Innov.*, **17**, No. S1, 101–106 (2013).

16. L. Y. Sheng, F. Yang, T. F. Xi, et al., "Microstructure evolution and mechanical properties of Ni_3Al/Al_2O_3 composite during self-propagation high-temperature synthesis and hot extrusion," *Mater. Sci. Eng. A*, **555**, 131–138 (2012).

17. L. Y. Sheng, B. N. Du, B. J. Wang, et al., "Hot extrusion effect on the microstructure and mechanical properties of a Mg–Y–Nd–Zr alloy," *Strength Mater.*, **50**, No. 1, 184–192 (2018).

18. L. Y. Sheng, F. Yang, T. F. Xi, et al., "Microstructure and room temperature mechanical properties of NiAl–Cr(Mo)–(Hf, Dy) hypoeutectic alloy prepared by injection casting," *Trans. Nonferr. Met. Soc. China*, **23**, No. 4, 983–990 (2013).

19. K. Nagatsuka, S. Yoshida, A. Tsuchiy, and K. Nakata, "Direct joining of carbon-fiber–reinforced plastic to an aluminum alloy using friction lap joining," *Compos. Part B-Eng.*, **73**, 82–88 (2015).

20. L. Y. Sheng, F. Yang, T. F. Xi, et al., "Influence of heat treatment on interface of Cu/Al bimetal composite fabricated by cold rolling," *Compos. Part B-Eng.*, **42**, No. 6, 1468–1473 (2011).

21. A. Pramanik, A. K. Basak, Y. Dong, et al., "Joining of carbon fibre reinforced polymer (CFRP) composites and aluminium alloys – A review," *Compos. Part A-Appl. S.*, **101**, 1–29 (2017).

Received 15. 03. 2018